ACADEMIC PRESS

Available online at www.sciencedirect.com

SCIENCE DIRECT®

Journal of Sound and Vibration 260 (2003) 731–755

JOURNAL OF SOUND AND VIBRATION

www.elsevier.com/locate/jsvi

Optimum support characteristics for rotor–shaft system with preloaded rolling element bearings

K.C. Panda[a], J.K. Dutt[b,*]

[a] *CASD, 70 Acre Complex, VSSC, Trivandrum, Kerala 695022, India*

[b] *Department of Mechanical Engineering, IIT Kharagpur, Kharagpur 721302, West Bengal, India*

Received 4 April 2000; accepted 15 May 2002

Abstract

Preloading of rolling element bearings is often used to avoid clearance in the bearings and achieve precise dynamic requirement. Preloading gives rise to an expression of the restoring force, which is a non-linear function of the deformation of the rolling elements. In this paper, frequency-dependent optimum support characteristics have been found out by simultaneously minimizing the unbalance response (UBR) of the rotor and maximizing the stability limit speed (SLS) of a flexible horizontal rotor–shaft system comprising an unsymmetrically placed rotor disc placed on an elastic shaft mounted on preloaded rolling element bearings at the ends supported on viscoelastic polymeric supports. A sensitivity study of the UBR and SLS with respect to the support characteristics has been presented to have an idea about the permissible deviation of the support characteristics from the respective optimum, at any frequency. Thus, the sensitivity study helps the quality control man as well as the manufacturer of such supports to estimate the permissible deviation in the most sensitive frequency zones. The results presented in this work are in terms of non-dimensional parameters of the system and are, therefore, valid for any system under consideration.

1. Introduction

This paper is written as a complementary part to the authors' paper in Ref. [1], in which the concept of simultaneous minimization of the unbalance response (UBR) and the maximization of the stability limit speed (SLS) was introduced to obtain optimum frequency-dependent support characteristics for a rotor–shaft system supported on viscoelastic polymeric supports. The concept of slope control of the support characteristics w.r.t. the frequency of excitation was also introduced to obtain feasible polymeric support characteristics. Linearity of the stiffness function

*Corresponding author.
E-mail address: jkdutt@mech.iitkgp.ernet.in (J.K. Dutt).

0022-460X/03/$ - see front matter © 2002 Elsevier Science Ltd. All rights reserved.
PII: S0022-460X(02)01071-4

of the bearings was assumed in the paper primarily for the purpose of simplicity. In reality, under any condition of loading, i.e., preloaded, loose or normal, a rolling element bearing exhibits a restoring force which is a non-linear function of the deformation of the bearing elements [2–4]. Therefore, non-linearity of the restoring force or in other words, non-linearity of the stiffness function of the bearings has been assumed in this paper for more accurate analysis and completeness. The effect of preloading on rotor response has been investigated in this paper as this is often used in a rotor–shaft system to eliminate clearance, resulting in free plays in the bearings and to achieve precise dynamics requirements [5]. Preloading is carried out by relative displacement of the bearing rings. This generates an initial compressive strain in the rolling elements and as a result, the expression of the stiffness function, which is non-linear in non-preloaded condition, becomes more complicated. Expression of stiffness under preloaded condition, as a function of deformation of rolling elements is given in Ref. [2]. The non-linear analysis with rolling element bearings has been reported, out of many other references, in Refs. [6,7] but the effect of preloading was not considered. In this paper a linearization technique reported in Ref. [8] has been used. Recently, viscoelastic polymeric materials have been used extensively as mounts or supports for vibration control by virtue of the efficiency of such materials to dissipate vibratory energy. A good survey of many of the applications as well as the operational advantages has been reported in Ref. [9]. Dutt and Nakra [10] presented the efficiency of such supports in increasing the SLS of a rotor–shaft system in comparison with other supports. Refs. [1,11] have also shown that the frequency-dependent properties of the viscoelastic supports can be used with advantage to minimize the UBR and increase the SLS. Moreover, recent literature [12] reports that tailor made mechanical properties can be generated using polymers. In this work, therefore, the viscoelastic polymeric supports are chosen. A sensitivity analysis has been reported at last to have an idea about the percentage deviation, i.e., increment of the UBR and decrement of SLS from the respective optimum at a particular frequency of excitation. The advantage of such an analysis is two-fold. Firstly, though the best support characteristics can be found out theoretically, it may not be possible to reproduce the characteristics exactly. Therefore, the sensitivity analysis will help the manufacturer or the quality control man to identify the most sensitive frequency zone and also get an idea about the permissible deviation of the support characteristics from the optimum, during manufacturing or checking the quality of such supports. Secondly, the support characteristics may also change due to change in temperature of the support elements. Hence, a sensitivity study will help to have a knowledge about the maximum possible deviation of UBR and SLS when the temperature changes in operating condition. The system considered in this paper is similar to the one considered in Ref. [1] but in this paper the horizontal mounting of the rotor–shaft and the preloaded rolling element bearings having non-linear stiffness function has been considered.

2. Analysis

2.1. Stiffness of preloaded bearings and linearization

2.1.1. Stiffness of preloaded bearing

The expression of stiffness of the preloaded bearings as a function of deformation of the rolling elements is obtained from Ref. [2]. Following these expressions, the stiffness of a preloaded

bearing can be written as

$$K_b(X_j) = d_1 - d_2\left|X_j^2\right| \quad \text{for } |X_j| \leqslant C_r, \tag{1}$$

$$K_b(X_j) = d_3|X_j|^{2/3} \quad \text{for } |X_j| > C_r, \tag{2}$$

where X_j is the deflection of the bearing along x direction. C_r is the amount of deflection due to preload and is shown in Fig. 2, and d_1, d_2 and d_3 are constants. The constants d_1, d_2 and d_3 can be evaluated by substituting $|X_j| = 0$ and C_r, in the above equations. Therefore, $K_b(0) = d_1$ and $K_b(Cr) = d_1 - d_2C_r^2 = d_3C_r^{2/3}$. Now the expression of stiffness can be written as

$$K_b(X_J) = K_b(0) - (K_b(0) - K_b(Cr))|X_j/C_r|^2 \quad \text{for } |X_j| \leqslant C_r, \tag{3}$$

$$K_b(X_J) = K_b(C_r)|X_j/C_r|^{2/3} \quad \text{for } |X_j| > C_r. \tag{4}$$

2.1.2. Non-dimensionalization

Non-dimensionalization of Eqs. (3) and (4) has been carried out by using the following parameters:

$$c_r = C_r/e_u, \quad x_j = X_j/e_u, \quad \beta_0 = K_b(0)/K^*, \quad \beta_{cr} = K_b(C_r)/K^*, \quad \beta_b = K_b(X_j)/K^*,$$

where $K^* = 3EII/(l_1^2l_2^2)$ is the stiffness of the shaft. Now Eqs. (3) and (4) can be written as

$$\beta_b(x_j) = \beta_0 - (\beta_0 - \beta_{cr})|x_j/c_r|^2 \quad \text{for } |x_j| \leqslant c_r, \tag{5}$$

$$\beta_b(x_j) = \beta_{cr}|x_j/c_r|^{2/3} \quad \text{for } |x_j| > c_r. \tag{6}$$

2.1.3. Linearization

The non-dimensional bearing stiffness, expressed in Eqs. (5) and (6) depend on the deformation of the rolling elements, and therefore gives rise to the restoring force varying non-linearly with the deformation of the rolling elements. The non-linear equations are difficult to handle for further analysis. Therefore, a linearization technique reported in Ref. [8] has been used to find the expression of linearized stiffness. The equivalent linearized stiffness has been used in the subsequent analysis. From Eqs. (5) and (6) the displacement-dependent restoring force can be expressed in the form

$$f_b(x_j) = \beta|x_j|^{n-1}x_j, \tag{7}$$

where f_b denotes the non-dimensional restoring force and 'n' is the index of non-linearity. Considering β_{bl} as the non-dimensional linearized stiffness it is possible to construct a non-dimensional error function of the stiffness and from the same a non-dimensional error function of the force experienced by the bearing by multiplying the non-dimensional error function of stiffness by the non-dimensional deformation parameter X_j. The non-dimensional error function of the restoring force is given by

$$\langle e \rangle = \beta_{bl}x_j - \beta|x_j|^{n-1}x_j. \tag{8}$$

Taking care of the changes in sign, it will be convenient to consider the square of the error function

$$\langle e^2 \rangle = (|\beta_{bl} x_j - \beta| |x_j|^{n-1} x_j|)^2, \tag{9}$$

where β_{bl} has been found out by the least square technique, i.e., by minimizing the integral of $\langle e^2 \rangle$, calculated over one full cycle of period T_s of the shaft, with respect to β_{bl}. Integrating $\langle e^2 \rangle$ first over T_s, we get

$$\langle \varepsilon^2 \rangle = \oint_{T_s} (|\beta_{bl} x_j - \beta |x_j|^{n-1} x_j|)^2 \, \mathrm{d}\tau. \tag{10}$$

Minimizing $\langle \varepsilon^2 \rangle$ w.r.t. β_{bl}, i.e., by setting $\partial \langle \varepsilon^2 \rangle / \partial \beta_{bl} = 0$ and using the fact that $|x_j|^2 = x_j \bar{x}_j$ (where $\bar{x}_j$ is the complex conjugate of X_j) we get

$$\beta_{bl} = \frac{\oint_{T_s} \beta |x_j|^{n+1} \, \mathrm{d}\tau}{\oint_{T_s} |x_j|^2 \, \mathrm{d}\tau}, \tag{11}$$

where x_j as in the case of a linear system has two parts, a harmonic and a horizontal part. So

$$x_j = x_{j,h} \mathrm{e}^{\mathrm{i}\omega t} + x_{j,g}, \tag{12}$$

where $x_{j,h}$ and $x_{j,g}$ are the complex amplitudes of the harmonic and the gravitational parts, respectively, and 'ω' is the whirl frequency of the rotor disc. Substituting Eq. (12) into Eq. (11) and with some more algebraic simplifications, β_{bl} can be obtained as

$$\beta_{bl} = \beta \left[|x_{j,h}|^2 + |x_{j,g}|^2 \right]^{(n-1)/2} \left[1 + \frac{(n^2-1)}{4} \frac{\left(|x_{j,h}| |x_{j,g}| \right)^2}{\left(|x_{j,h}|^2 + |x_{j,g}|^2 \right)} + \cdots \right]. \tag{13}$$

The details of the derivation leading to Eq. (13) can be obtained from Ref. [8]. The dimensional linearized stiffness

$$(K_{b,lin}) = \beta_{bl} K^*. \tag{14}$$

In the derivation of dimensional equations of motion $K_{b,lin}$ has boon used for the left and right bearings with indices L and R, respectively, i.e., $(K_{b,lin})_L$ and $(K_{b,lin})_R$ refer to linearized stiffness of the bearing for left and right bearings, respectively. In this work as the rotor disc is mounted unsymmetrically the value of stiffness for left bearing will be different than that of right bearing and these stiffnesses are calculated by using the deflections of left and right side bearings, respectively.

2.2. Assumptions and equations of motion

2.2.1. Assumptions

The system has been assumed to comprise of a single rotor disc placed horizontally on a linearly elastic, massless shaft having preloaded rolling element bearings at the ends supported on viscoelastic supports. Viscous form of internal damping has been assumed for modelling the shaft. Though preloading of rolling element bearings give rise to restoring forces varying non-linearly with the deformation of the rolling elements, the process of linearization given in Section 2.1.3 has

been used to obtain the linearized stiffness. Damping in rolling element bearing is negligible and has not been considered. Gyroscopic effect due to non-central locations of the rotor disc, mass of the supports have also been taken into account for deducing the equations of motion. Support mass has been considered while formulating the equations of motion. The viscoelastic support has been assumed to be a linear viscoelastic solid and has been modelled using a four-element model.

2.2.2. Equations of motion

The system considered for the analysis is shown in Fig. 1. With the expressions of the linearized stiffness already at hand the same has been used to find out the equations of motion. The equations have been found out from Lagrange's principle as was followed in Ref. [1]. The expression for kinetic energy T, potential energy V are given as

$$T = \tfrac{1}{2}[M_2\dot{X}_2^2 + M_2\dot{Y}_2^2 + I_P\omega^2 + I_t\dot{\theta}^2 + I_t\dot{\phi}^2 + 2I_p\omega\dot{\phi}\theta] + M_1\dot{X}_{1L}^2 + M_1\dot{Y}_{1L}^2 + M_1\dot{X}_{1R}^2 + M_1\dot{Y}_{1R}^2 + M_3\dot{X}_{3L}^2 + M_3\dot{Y}_{3L}^2 + M_3\dot{X}_{3R}^2 + M_3\dot{Y}_{3R}^2, \quad (15)$$

$$V = \tfrac{1}{2}[C_{22}(\theta-\alpha)^2 + C_{22}(\phi-\beta)^2 - 2C_{12}(\theta-\alpha)Y_s - 2C_{12}(\phi-\beta)X_s + (K_{b,lin})_L X_{JL}^2 + (K_{b,lin})_L Y_{JL}^2 + (K_{b,lin})_R X_{JR}^2 + (K_{b,lin})_R Y_{JR}^2 + K_1 X_{1L}^2 + K_1 Y_{1L}^2 + K_1 X_{1R}^2 + K_1 Y_{1R}^2 + K_2(X_{1L}-X_{3L})^2 + K_2(Y_{1L}-Y_{3L})^2 + K_2(X_{1R}-X_{3R})^2 + K_2(Y_{1R}-Y_{3R})^2], \quad (16)$$

where C_{12} represents force/angular deflection or moment/deflection of the shaft at the rotor disc location and is derived as $K^*l(e_2-e_1)$. C_{22} represents angular stiffness of the shaft at the rotor disc location (moment/angular deflection) and is derived as $K^*l^2(e_1-e_2)$. K^* is given by $3EIl/l_1^2l_2^2$, 'E' is

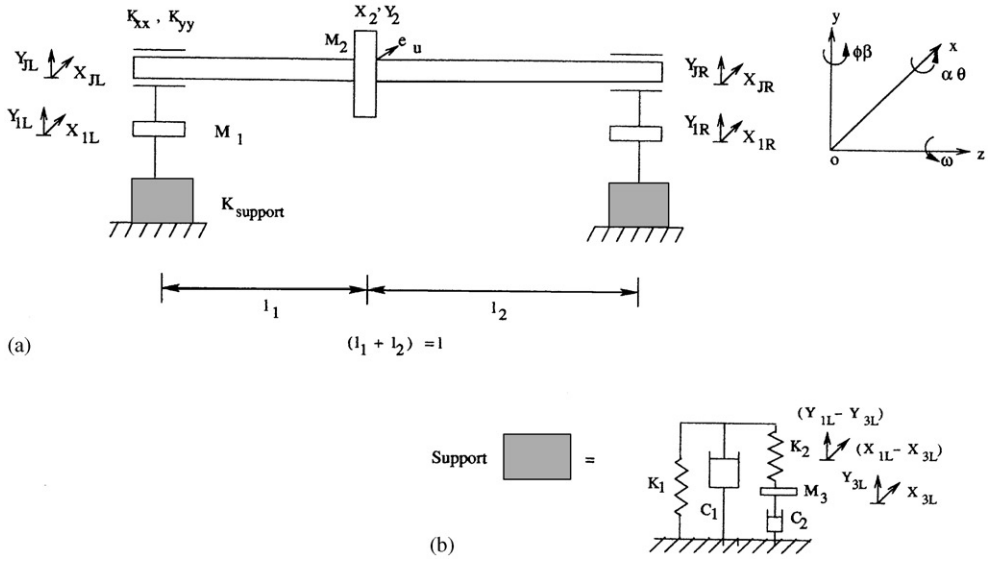

Fig. 1. (a) System diagram with preloaded bearings and (b) the support, its model with the displacements of the elements in the X and Y directions.

the modulus of elasticity and 'I' is the sectional moment of inertia of shaft. Subscripts L and R are for left and right sides, respectively. The absolute displacements $[X_2, Y_2]$ $[X_{1L}, Y_{1L}, X_{1R}, Y_{1R}]$ and $[X_{3L}, Y_{3L}, X_{3R}, Y_{3R}]$ are of the rotor disc, support mass at left and right ends and the displacements of the secondary dampers at left and right ends, respectively. The displacements $\{X_{JL}, Y_{JL}, X_{JR}, Y_{JR}]$ are relative displacements of bearings at left and right sides, respectively, θ and ϕ are the absolute angular deflections of the rotor disc axis due to elastic deformation of the shaft about X- and Y-axis, respectively, and the angular orientations α and β are the absolute orientation of the rotor axis with Z-axis, considering the shaft as a rigid body in, YZ and XZ plane, respectively. The terms $(X_{1L}-Y_{3L})$ and $(X_{1R}-Y_{3R})$ are absolute displacements of secondary springs at left and right sides, respectively. The expression for dissipation function D can be written as

$$D = C_i[(\dot{X}_s^2 + \dot{Y}_s^2)/2 + \omega(Y_s\dot{X}_s - X_s\dot{Y}_s)] + \tfrac{1}{2}C_1[\dot{X}_{1L}^2 + \dot{Y}_{1L}^2 + \dot{X}_{1R}^2 + \dot{Y}_{1R}^2] + \tfrac{1}{2}C_2[\dot{X}_{3L}^2 + \dot{Y}_{3L}^2 + \dot{X}_{3R}^2 + \dot{Y}_{3R}^2], \tag{17}$$

where α, β, X_s, Y_s can be written as

$$\alpha = (X_{JR} + X_{1R} - X_{JL} - X_{1L})/L, \tag{18}$$

$$\beta = (Y_{JR} + Y_{1R} - Y_{JL} - Y_{1L})/L, \tag{19}$$

$$X_s = X_2 - (X_{JL} + X_{1L})e_2 - (X_{JR} + X_{1R})e_1, \tag{20}$$

$$Y_s = Y_2 - (Y_{JL} + Y_{1L})e_2 - (Y_{JR} + Y_{1R})e_1. \tag{21}$$

Considering the bearing to have *only direct stiffness and negligible damping* the equations of motion have been found out, and given in Appendix A. Where terms with subscript "h" denotes the harmonic component and those with subscript "g" denotes gravitational components of the respective displacement. For example any displacement $X_i = X_{ih} + X_{ig}$, where X_i is generic name for $X_1, X_2, X_s, X_{1L}, X_{1R}, X_{2L}, X_{2R}, X_{3L}, X_{3R}, X_{JL}, X_{JR}, Y_{1L}, Y_{1R}, Y_{2L}, Y_{2R}, Y_{3L}, Y_{3R}, Y_{JL}, Y_{JR}, \theta, \phi, \alpha, \beta$.

3. Rotor response and stability limit speed

3.1. Finding the linearized stiffness

Before obtaining the rotor response the linearized bearing stiffness has to be found out for each operating speed. From Eq. (3) it is observed that for no deflection of the bearing elements, there is a particular value of the bearing stiffness. When the speed of the rotor increases, the elements deform and for the next operating speed the value of the bearing stiffness changes in a manner given in Eq. (13). Here, for calculating the bearing stiffness the deflection corresponding to previous step of operating speed is used in Eq. (13). Likewise the linearized stiffness value is calculated for each operating speed of the rotor. The value of the stiffness obtained in this way is an approximate one. A comparison between approximate linearized stiffness and the actual value of the stiffness for left bearing has been given in Fig. 2b. Seeing the equations in Appendix A.1 it may be found that forcing function is a harmonic function due to unbalanced excitation and a constant gravitational function act on the rotor–shaft system. So each displacement will found as a resultant of two components, a harmonic component and a gravitational component. Equating

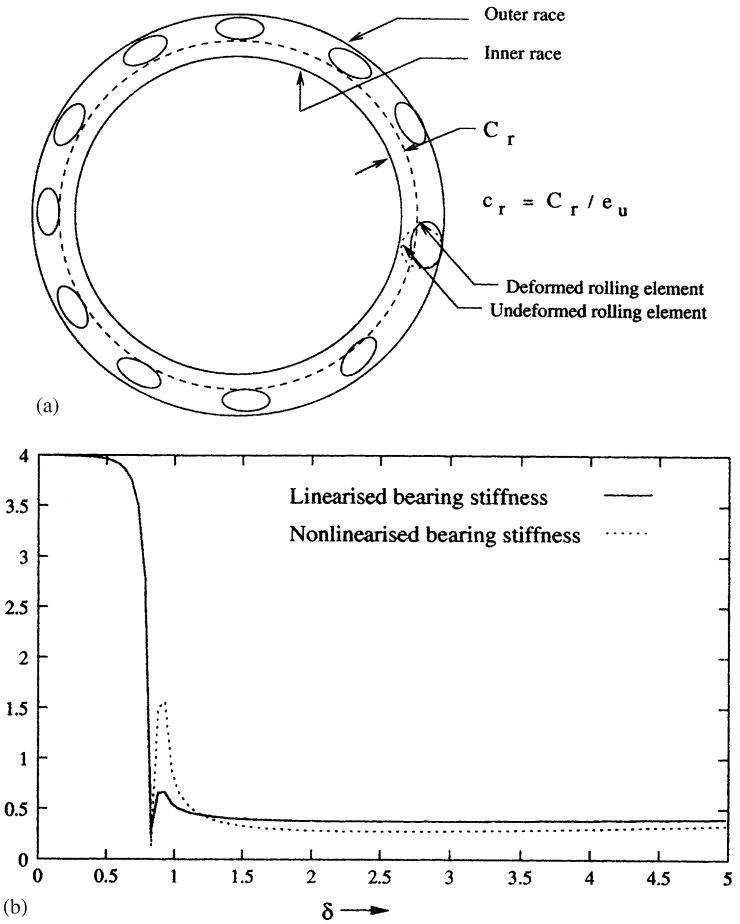

Fig. 2. (a) Sketch showing the deformation of the rolling element in the rolling element bearing and (b) linearized and nonlinearized bearing stiffness w.r.t. operating speed of the system.

the harmonic terms and the gravitational terms in the left side of the equations in Appendix A.1 to corresponding terms on the right-hand side will result in two sets of equations. Solution of the set of equation due to harmonic components and that for the gravitational components will give the harmonic and the gravitational components of displacements, respectively. The harmonic and gravitational components have to be superposed to get resultant generalized displacement vector $\{q\}$. The value of $\{q\}$ obtained in this method assumes the $K_{b,lin}$ value corresponding to the previous iteration of ω (as solution is obtained for each value of ω from zero to maximum operating speed). To get the exact solution for $\{q\}$ the set of non-linear equations for the system, as given in Appendix A.1, obtained with out isolating harmonic and gravitational parts has been solved using the numerical method of solving sets of non-linear equations as given in Ref. [13]. In this work the above numerical method of solution of non-linear equations has been used because, due to the presence of many variables and equations, it is not easy to solve the harmonic set of equations by substitution method to find out the $K_{b,lin}$ as a function of ω as was followed in

Ref. [8]. The use of linearization technique in this case only helps in providing a good initial guess to the sets of non-linear equations for quick convergence of the solution.

3.2. Harmonic components of generalized displacements

The harmonic part of generalized displacements (q_h) is found by solving the harmonic set of equations, obtained from equations in Appendix A.1. The harmonic components of the force along X and Y directions are $M_2 e_u \omega^2 \cos(\omega t)$ and $M_2 e_u \omega^2 \sin(\omega t)$, where e_u is the eccentricity at rotor disc and 't' is time in seconds. Considering the forces due to unbalance the equations of motion in dimensional form can be written as

$$[M]\{\ddot{Q}\} + [C]\{\dot{Q}\} + [K]\{Q\} = \{F_h\}, \tag{22}$$

where $[M]$, $[C]$, and $[K]$ are the mass, damping and stiffness matrices, respectively, and are square type in the present analysis. The force and displacement vectors $\{F_h\}$, $\{Q\}$ are column vectors and can be written as

$$\{F_h\} = [M_2 e_u \omega^2 \cos(\omega t), M_2 e_u \omega^2 \sin(\omega t), 0, 0, 0, 0, 0, 0, 0, 0, 0, 0, 0, 0, 0, 0]^{\mathrm{T}},$$

$$\{Q\} = [X_{2,h}, Y_{2,h}, X_{JL,h}, Y_{JL,h} X_{JR,h}, Y_{JR,h}, X_{1L,h}, Y_{1L,h}, X_{1R,h}, Y_{1R,h}, X_{3L,h}, Y_{3L,h}, X_{3R,h}, Y_{3R,h}, \phi_h, \theta_h]^{\mathrm{T}}.$$

The force vector can also be written as $\{Fh\} = \{f_h\} \mathrm{e}^{\mathrm{i}\omega t}$.

Assuming a harmonic solution $Q_i = q_{i,h} \mathrm{e}^{\mathrm{i}\omega t}$, for finding out steady state synchronous response, where Q_i is the ith element of $\{Q\}$, the equation of motion can be represented as

$$[-\omega^2[M] + \mathrm{i}\omega[C] + [K]]\{q_h\} = \{f_h\}. \tag{23}$$

Using the non-dimensional parameters $\delta = \omega/\omega_n$, $R = I_p/I_t$, $c = \sqrt{K^*/C_2^2}\sqrt{I_t/M_2}$, $\alpha_1 = M_1/M_2$, $\alpha_2 = M_3/M_2$, $\zeta_i = C_i/C_c$, $\beta_1 = K_1/K^*$, $\beta_2 = K_2/K^*$, $\zeta_1 = C_1/C_c$, $\zeta_2 = C_2/C_c^*$, $\beta_{bl} = K_{bl}/k$ the forced non-dimensional equations of motion for harmonic displacements can be found out, from Appendix A.2, in a similar way followed for finding dimensional set of equations explained in Section 3.1. The set of Eq. (23) can be expressed in the form

$$[A]\{q_h\} = \{f_h\}, \tag{24}$$

where $\{q_h\}$ and $\{f_h\}$ denote harmonic components of the generalized displacement and the amplitude of force vector, respectively.

3.3. Gravitational components of generalized displacements

The gravitational components of generalized displacements can be obtained from Appendix A.1 by solving the set of equations due to gravitational components. In gravitational components of displacements the time derivatives of the displacements will be zero, since these displacements are constants but the gravitational components of displacements will be both along X and Y directions. The displacements along X direction exists due to the presence of internal damping in the rotor–shaft. The generalized displacements due to gravity can be written as $\{q_g\}$. Now the total rotor response can be obtained by superimposing the gravitational component on which can

be written as

$$\{q\} = \{q_h\} + \{q_g\}. \tag{25}$$

3.4. Rotor response

The superimposed solution obtained, in the above section, by superimposing harmonic and gravitational part of the displacement vectors are the approximate ones and used for the initial guess for the exact solution. The exact solution for a horizontal system subjected to harmonic loading due to unbalance can be found out by solving the sets of non-linear equations given in Appendix A. After getting the generalized rotor response the UBR can be obtained as

$$z_2 = [\text{Real}(q_1 e^{i\omega t}) + i\,\text{Real}(q_2 e^{i\omega t})]. \tag{26}$$

The non-dimensional UBR amplitude can be written as

$$\mathbf{RD} = |\mathbf{z}_2|/\mathbf{e_u}. \tag{27}$$

3.5. Stability limit

To find the SLS of the system, Eq. (22) can be written in state space form and the free vibration problem then leads to

$$\begin{bmatrix} 0 & M \\ M & 0 \end{bmatrix} \begin{Bmatrix} \ddot{q} \\ \dot{q} \end{Bmatrix} + \begin{bmatrix} -M & 0 \\ C & K \end{bmatrix} \begin{Bmatrix} \dot{q} \\ q \end{Bmatrix} = \{0\},$$

which are of the form

$$[A1]\{\dot{u}\} + [A2]\{u\} = \{0\}, \tag{28}$$

where

$$\begin{bmatrix} \dot{q} \\ q \end{bmatrix} = \{u\} \quad \text{and} \quad \begin{bmatrix} \ddot{q} \\ \dot{q} \end{bmatrix} = \{\dot{u}\}.$$

For finding the SLS at a particular operating speed, the value of bearing stiffness is assumed to be the linearized value corresponding to the same operating speed. After converting the equations into the form as in Eq. (28) the stability analysis has been done by examining the sign of the real part of the eigenvalues, which are complex in general, for each step of increment of speed, using the EISPACK Subroutine [14]. The non-dimensional SLS is represented by *DLIMIT*:

$$DLIMIT = \frac{\text{Stability limit speed}}{\text{Fundamental undamped natural frequency of the system } (\omega_n)}. \tag{29}$$

4. Optimization

The separate parametric analysis for *RD* and *DLIMIT* shows that for each parameter there exists an optimum point. After determining the non-dimensional unbalance response amplitude

(*RD*) and stability limit speed (*DLIMIT*), which are functions of non-dimensional *support parameters*, i.e., β_1, β_2, ζ_1, ζ_2, optimization has been carried out in order to predict the optimum non-dimensional *support characteristics*, i.e., K_{sn} and η, the expressions for which are given below:

$$K_{sn} = \frac{\beta_1\beta_2^2 + 4\delta^2\zeta_2^2(\beta_1 + \beta_2)}{\beta_2^2 + 4\delta^2\zeta_2^2}, \tag{30}$$

$$\eta = \frac{2\delta\beta_2^2(\zeta_1 + \zeta_2) + 8\zeta_1\zeta_2^2\delta^3}{\beta_1\beta_2^2 + 4\delta^2\zeta_2^2(\beta_1 + \beta_2)}. \tag{31}$$

As reported in the author's paper [1] two schemes for optimization have been tested.

Scheme-I

OBJECTIVE = minimize (*RD*)

CONSTRAINTS: (a) Support deflection should be within limits, (b) other space limitations should not be violated, (c) loss factor of the support (η) should be within achievable limits, and (d) constraints for support characteristics

Scheme-II

In this scheme to maximize the SLS while minimizing the UBR an objective function has been formulated by taking the difference of *RD* and *DLIMIT*, i.e., (*RD* − *DLIMIT*).

OBJECTIVE = minimize (*RD* − *DLIMIT*)

CONSTRAINTS: Same as those considered in Scheme-I

η is the loss factor of the viscoelastic support. The characteristics of viscoelastic materials are given in Ref. [15]. It is found that the in-phase stiffness increases uniformly and monotonically with frequency while the variation of loss factor with frequency is uniform. Again it is observed that more often than not the maximum value of the loss factor is $\leqslant 1$. Hence, constraint for loss factor used in this work is, $\eta \leqslant 1$. However, no constraint on space restrictions or other system constraints have been considered in this work. They can definitely be taken care of under the schemes proposed. The objective function has been optimized by an optimization subroutine, which optimizes the function by gradient method [16]. The objective function is optimized for each stepwise increment of the speed of rotation, to predict values for support parameters for that speed.

5. Importance of slope control

5.1. Examples

Fig. 3a shows the variation of *RD* and *DLIMIT* w.r.t. δ, for rotor–shaft system with preloaded rolling element bearings at the ends using optimization Scheme-II. The system parameters considered for analysis are: $\zeta_i = 0.03$, $\alpha_i = 0.4$, $\alpha_2 = 0.00667$, $\beta_0 = 4$, $\beta_{cr} = 0.5$, $c_r = 0.5$, $e = 0.4$, $\gamma = 0.1$. Fig. 3b shows the variation of non-dimensional support characteristics (K_{sn} and η) for the

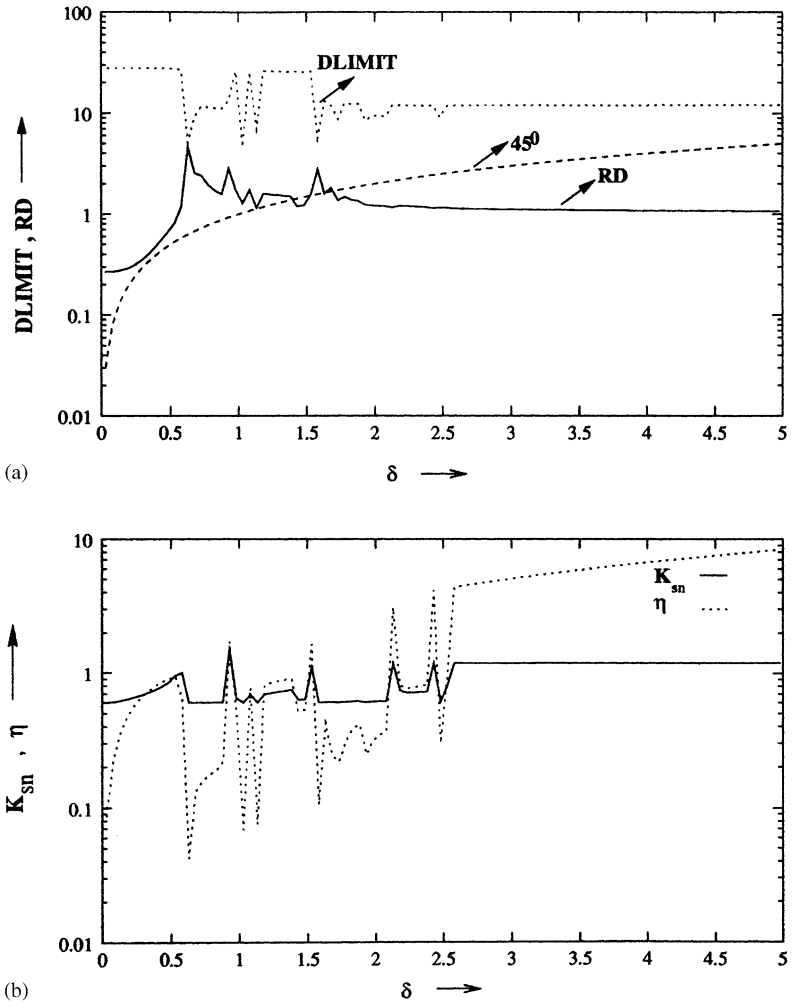

Fig. 3. (a) Variation of UBR and SLS with out using slope control (when Scheme-II optimization is followed) and (b) variation of K_{sn} and η with out slope control.

respective cases. From Fig. 3b it is observed that the variation of support characteristics include sudden changes as the respective support parameters vary suddenly. Obviously, it is difficult, if not impossible to reproduce the support characteristics with sudden variations, using a polymeric material for which the characteristics are smooth. Therefore, a slope control technique for support parameters as well as support characteristics has been used in this work.

5.2. Slope control

The starting values of support parameters are taken to be at their lower limits. During the next increase in speed the optimization subroutine predicts the optimum values of support parameters

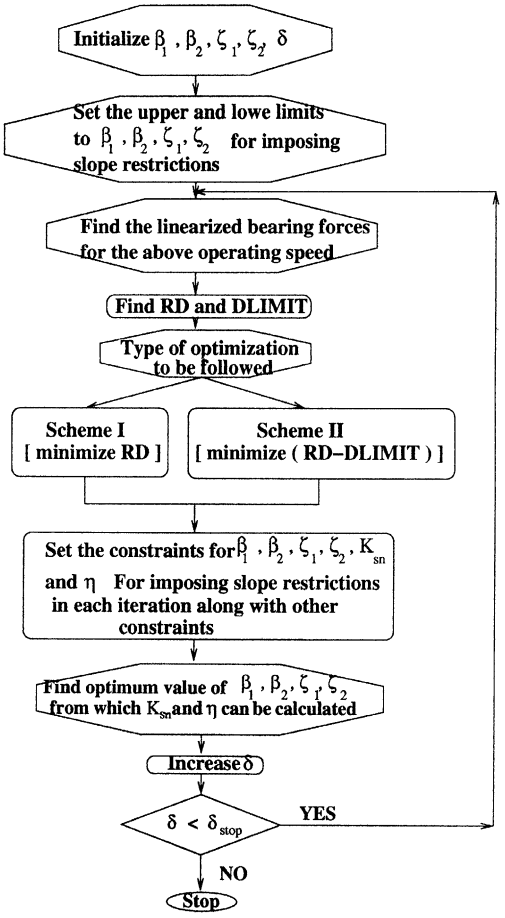

Fig. 4.

β_1, β_2, ζ_1, ζ_2 from which support characteristics K_{sn} and η can be found using the Eqs. (30) and (31). To predict the support characteristics, which vary smoothly, constraints have been put on the K_{sn} and η curves plotted w.r.t. δ such that their slopes always lie within 0–30°, a value chosen tacitly. The process of slope control used for two types of optimization schemes can be best explained by the flow chart given in Fig. 4.

6. Sensitivity analysis

6.1. The use of sensitivity

In reality, it may not be possible for the manufacture to produce the exact values of support stiffness and damping at a particular frequency, for the optimum performances when a passive

frequency-dependent support is designed. Hence it is quite useful to have at hand the expected results, when there is a deviation from the predicted value. It helps the designers:

- To find out the most sensitive frequency zones, where excess care is required to reproduce the predicted support characteristics.
- To find out the percentage variation in the performance of the system, in terms of *RD* and *DLIMIT*, if the actual support characteristics deviate from the predicted optimum values.
- To have an idea about the bound of the response and stability limit due to change in temperature of the support as polymeric characteristics are temperature dependent.

From earlier sections it is observed that *RD*, *DLIMIT*, K_{sn} and η each is a function of β_1, β_2, ζ_1 and ζ_2. Hence we can express the percentage variation of *RD* and *DLIMIT* for unit percentage variation of K_{sn} and η each and these are nothing but the sensitivity of *RD* and *DLIMIT* w.r.t. K_{sn} and η. The sensitivity of *RD* and *DLIMIT* are found for each step wise increment of operating speed only after finding the optimum values of K_{sn} and η for each operating speed. The mathematical expressions are as follows:

6.2. The process of finding the sensitivity

Sensitivity as explained in any text on control theory can be expressed mathematically as the rate of change of an objective function w.r.t. a parameter. Therefore the sensitivity of *RD* and *DLIMIT* w.r.t. K_{sn} and η can found out by calculating $\partial(RD)/\partial K_{sn}, \partial(DLIMIT)/\partial K_{sn}$, $\partial(RD)/\partial\eta, \partial(DLIMIT)/\partial\eta$. Supposing $RD = f_1(\beta_1, \beta_2, \zeta_1, \zeta_2)$, $DLIMIT = f_2(\beta_1, \beta_2, \zeta_1, \zeta_2)$, $K_{sn} = f_3(\beta_1, \beta_2, \zeta_1, \zeta_2)$, $\eta = f_4(\beta_1, \beta_2, \zeta_1, \zeta_2)$:

$$\frac{\partial(RD)}{\partial\beta_1} = \frac{\partial(RD)}{\partial K_{sn}}\frac{\partial K_{sn}}{\partial\beta_1} + \frac{\partial(RD)}{\partial\eta}\frac{\partial\eta}{\partial\beta_1}, \tag{32}$$

$$\frac{\partial(RD)}{\partial\beta_2} = \frac{\partial(RD)}{\partial K_{sn}}\frac{\partial K_{sn}}{\partial\beta_2} + \frac{\partial(RD)}{\partial\eta}\frac{\partial\eta}{\partial\beta_2}, \tag{33}$$

$$\frac{\partial(DLIMIT)}{\partial\beta_1} = \frac{\partial(DLIMIT)}{\partial K_{sn}}\frac{\partial K_{sn}}{\partial\beta_1} + \frac{\partial(DLIMIT)}{\partial\eta}\frac{\partial\eta}{\partial\beta_1}, \tag{34}$$

$$\frac{\partial(DLIMIT)}{\partial\beta_2} = \frac{\partial(DLIMIT)}{\partial K_{sn}}\frac{\partial K_{sn}}{\partial\beta_2} + \frac{\partial(DLIMIT)}{\partial\eta}\frac{\partial\eta}{\partial\beta_2} \tag{35}$$

solving Eqs. (32)–(35) $\partial(RD)/\partial K_{sn}, \partial(RD)/\partial\eta$ and $\partial(DLIMIT)/\partial K_{sn}, \partial(DLIMIT)/\partial\eta$ are calculated, respectively. For example,

$$\frac{\partial(RD)}{\partial K_{sn}} = \frac{\dfrac{\partial\eta}{\partial\beta_2}\dfrac{\partial(RD)}{\partial\beta_1} - \dfrac{\partial\eta}{\partial\beta_1}\dfrac{\partial(RD)}{\partial\beta_2}}{\dfrac{\partial K_{sn}}{\partial\beta_1}\dfrac{\partial\eta}{\partial\beta_2} - \dfrac{\partial\eta}{\partial\beta_1}\dfrac{\partial K_{sn}}{\partial\beta_2}}, \tag{36}$$

which can also be written in percentage form, given below:

$$\frac{\partial(RD).K_{sn}}{\partial K_{sn}.(RD)} = \frac{\dfrac{\partial\eta}{\partial\beta_2}\dfrac{\beta_2}{\eta}\dfrac{\partial(RD).\beta_1}{\partial\beta_1.(RD)} - \dfrac{\partial\eta}{\partial\beta_2}\dfrac{\beta_1}{\eta}\dfrac{\partial(RD).\beta_2}{\partial\beta_2.(RD)}}{\dfrac{\partial K_{sn}}{\partial\beta_1}\dfrac{\beta_1}{K_{sn}}\dfrac{\partial\eta}{\partial\beta_2}\dfrac{\beta_2}{\eta} - \dfrac{\partial\eta}{\partial\beta_1}\dfrac{\beta_1}{\eta}\dfrac{\partial K_{sn}}{\partial\beta_2}\dfrac{\beta_2}{K_{sn}}}. \tag{37}$$

7. Results and discussion

7.1. Effects of preloading

The Figs. 5a–c present the effect of preloading on *RD*, stiffness of left bearing $(\beta_{b,lin})_L$ and stiffness of right bearing $(\beta_{b,lin})_R$, respectively. Higher value of c_r signifies that the amount of preloading is more. Figs. 5b and c indicate that for higher value of preloading the bearing stiffness (or reaction forces) are less, it is because higher value of preloading will reduce the radial action force (from the shaft) on the balls of the bearing. Hence, the reaction forces are less. From Tables 1 and 2 it is observed that when c_r value increases, there is a gradual increase in *RD* and after a particular value of c_r *RD* decreases and increases again. This indicates that there exists an optimum value of c_r corresponding to which *RD* is minimum. The effects have been studied for systems with rigid supports as well as with viscoelastic supports. The system parameters for rigid support are $\alpha_1 = 0.4$, $\alpha_2 = 0.00667$, $\beta = 4$, $\zeta_i = 0.005$, $\beta_{cr} = 0.5$, $c_r = 0.5$, $e = 0.4$, $\gamma = 0.1$.

For the system with viscoelastic supports the system parameters are $\alpha_1 = 0.4$, $\alpha_2 = 0.00667$, $\zeta_1 = 0.025$, $\beta = 4$, $\zeta_i = 0.005$, $\beta_1 = 0.5$, $\beta_2 = 0.25$, $\zeta_2 = 0.02$, $\beta_{cr} = 0.5$, $c_r = 0.5$, $e = 0.4$, $\gamma = 0.1$.

7.2. Optimization results

In this section the optimum support characteristics and the corresponding *RD* and *DLIMIT* as functions of δ will be presented using both optimization Schemes-I and -II. For this analysis the values of system parameters chosen are: $\zeta_i = 0.006$, $\alpha_1 = 0.4$, $\alpha_2 = 0.00667$, $\beta_0 = 4$, $\beta_{cr} = 0.25$, $c_r = 0.5$, $e = 0.4$, $\gamma = 0.1$.

Figs. 6a and c show, respectively, the variations of *RD* and *DLIMIT* w.r.t. δ for optimization Schemes-I and -II with the concept of slope control applied to support characteristics. Fig. 6b and d present the respective support characteristics. From Figs. 6a and c it is observed that optimization Scheme-II undoubtedly improves the SLS in comparison to optimization Scheme-I. At the same time, the first peak of UBR diminishes to a great extent. The reduction of UBR, as observed in this case, is due to the choice of Optimization Scheme-II. It may be noted that the system has two sources viz the internal damping forces in the shaft and the non-linear restoring forces in the bearings, which may cause instability. The former being viscous in nature is proportional to the amplitude of deflection of the rotor disc in the case of synchronous response but the latter varies non-linearly with the deformation of the rolling elements. Therefore, the optimization Scheme-II, which finds out the support characteristics by minimizing the UBR and maximizing the SLS simultaneously, provides a better arrangement to dissipate the vibratory

energy. Hence the response reduces. This also shows that Scheme-II is a better method of obtaining support characteristics as concluded in Ref. [1]. It is also observed that the support characteristics are fairly smooth and do not involve any sudden change. This is the advantage of slope control technique.

7.3. Sensitivity results

Figs. 7a–d show the sensitivities of *RD* and *DLIMIT* to the support characteristics K_{sn} and η. Figs. 7a and c show the sensitivity of *RD* to K_{sn} and η for Schemes-I and -II, respectively, and

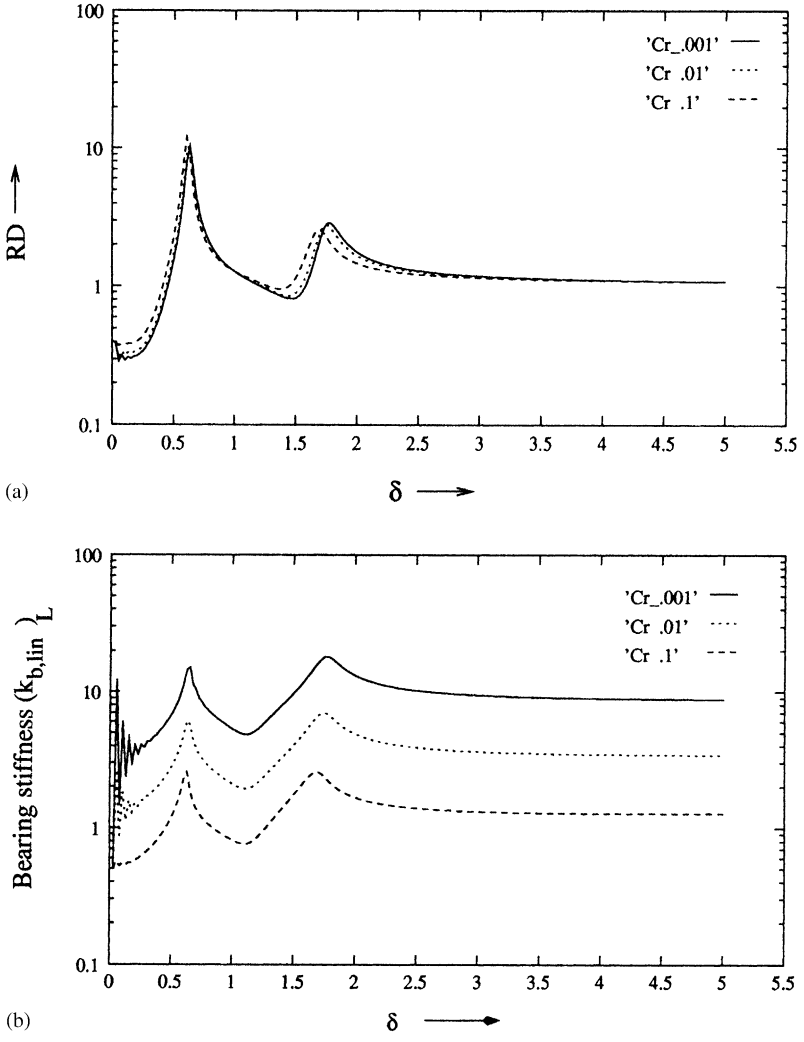

Fig. 5. (a) Effect of different C_r on *RD*, (b) effect of different C_r on bearing stiffness, and (c) effect of different C_r on right stiffness.

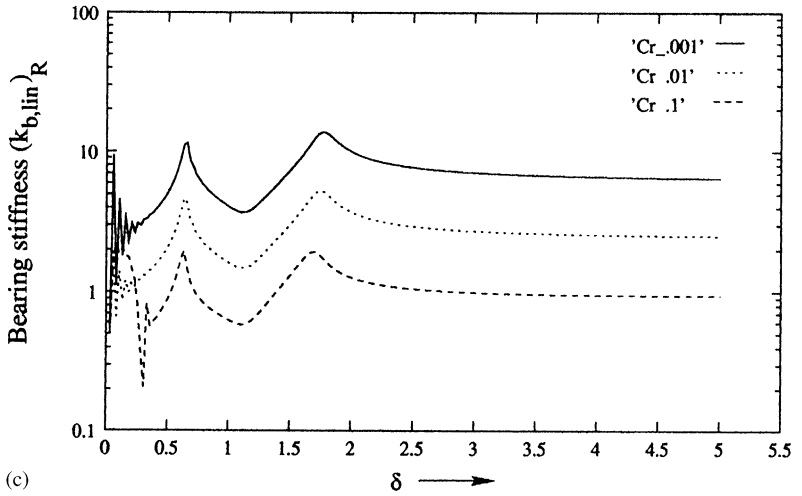

(c)

Fig. 5 (*continued*).

Table 1

c_r	0.001	0.01	0.1	0.3	1	2	4	5	6	10
RD at 1st peak	45.92	214.4	152.29	272	6.7	36	105	147.61	83.3	54
RD at 2nd peak	—	—	—	—	2.23	5.35	10	11.17	11.7	11.97

Table 1

c_r	0.001	0.01	0.1	0.3	1	2	4	5	6	10
RD at 1st peak	45.92	214.4	152.29	272	6.7	36	105	147.61	83.3	54

Table 2

c_r	0.001	0.01	0.1	0.3	1	2	4	5	6	10
RD at 1st peak	13.37	10.29	11.90	14.23	10.05	9.80	9.89	9.89	9.90	9.91
RD at 2nd peak	2.87	2.78	2.54	2.35	2.24	2.63	2.66	2.66	2.67	2.67

Table 2

c_r	0.001	0.01	0.1	0.3	1	2	4	5	6	10
RD at 1st peak	13.37	10.29	11.90	14.23	10.05	9.80	9.89	9.89	9.90	9.91

Figs. 7b and d show the sensitivity of *DLIMIT* for the respective schemes. Sensitivity at a particular non-dimensional frequency δ, means, the percentage deviation (positive or negative) of the quantity, e.g., *RD* or *DLIMIT* from the corresponding optimum values of K_{sn} (or η) at frequency due to $+1\%$ change in the value. It may be noticed from each of Figs. 7a–d that outside a band of frequencies, the value of sensitivity is very low, or *RD* and *DLIMIT* are insensitive to changes in support characteristics. So with in this frequency band, the support characteristics should be as near the optimum values as possible in order to obtain the optimum performance in terms of *RD* and *DLIMIT*.

It may also be noticed from Figs. 7a and c, that *RD*, in the case of Scheme-II, is much less sensitive to the changes in support characteristics, and thus, Scheme-II provides more realistic support characteristics.

In general it may be noticed that, both *RD* and *DLIMIT* are very sensitive to K_{sn} in comparison with η. This is so, because, in reality, the optimization process aims at positioning the system natural frequencies in such a way that resonance can be avoided. So, minor change in the loss factor does not create much change, in the values of *RD* or *DLIMIT*. It may be noticed that, a negative deviation in the value of *RD* at a particular frequency or a negative sensitivity of *RD* and a positive sensitivity for *DLIMIT* are beneficial, as in that case the unbalanced response amplitude decreases and the SLS increases. In view of the definition of sensitivity given above,

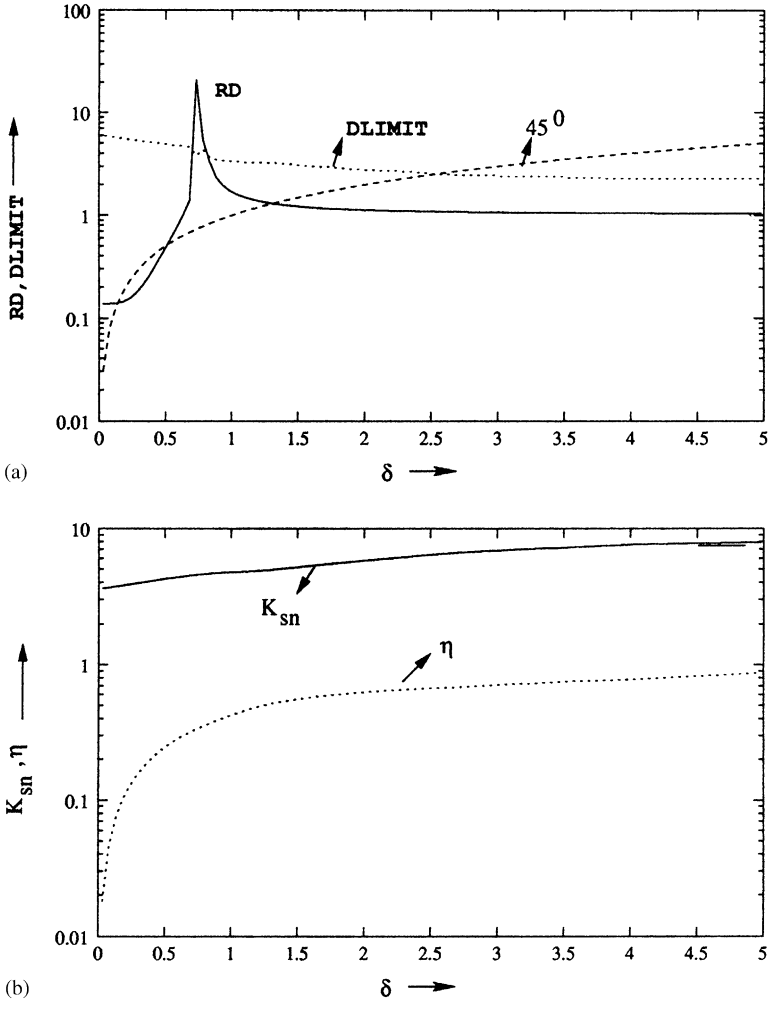

Fig. 6. (a) UBR and SLS when *RD* is minimized or Scheme-I is followed, (b) Support characteristics when Scheme-I is followed, (c) UBR and SLS when *RD-DLIMIT* is minimized or Scheme-II is followed, and (d) support characteristics when Scheme-II is followed.

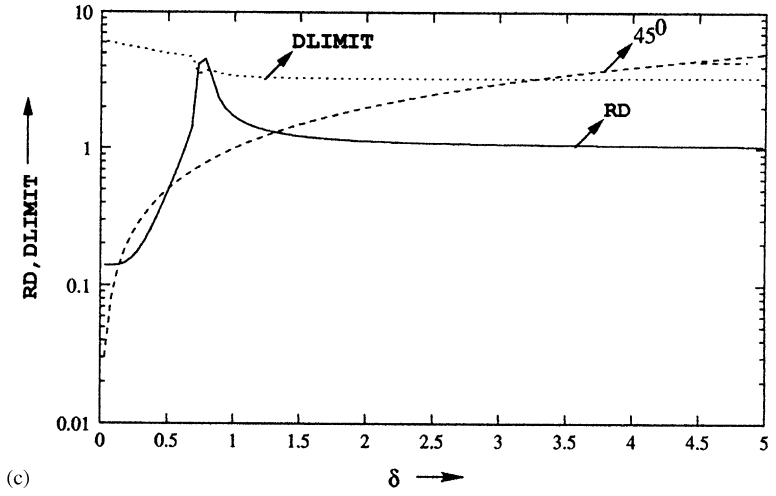

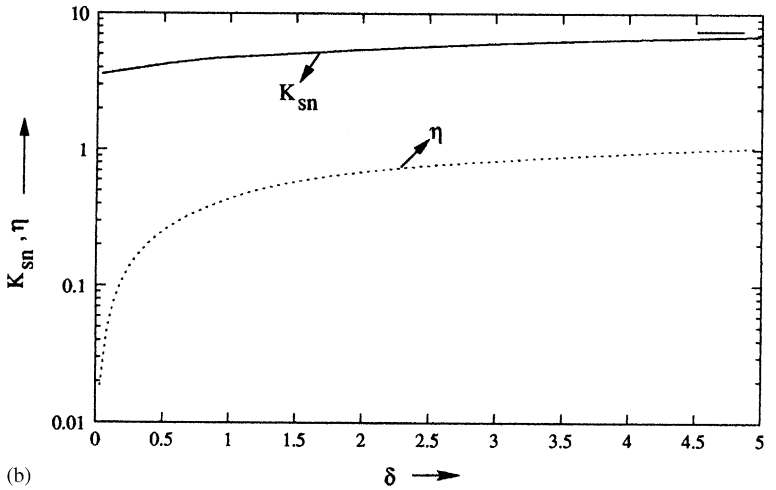

Fig. 6 (*continued*).

deviation of the values of K_{sn} and η in the negative direction are tolerable, in the most sensitive frequency band as it will reduce *RD* and increase *DLIMIT*.

8. Conclusions

- Minimization of UBR as well as maximization of SLS is essential for designing better supports.
- Slope control technique is very useful in predicting a feasible support characteristics.
- Sensitivity results predicts the most sensitive frequency zone where care should be taken while selecting/designing a support. It also gives an idea about the permissible deviation, of the support characteristics, both in magnitude and sense.

Appendix A. Resultant equations of motion for rotor–shaft system

A.1. In dimensional form

$$M_2(\ddot{X}_{2h} + \ddot{X}_{2g}) + K_s(X_{sh} + X_{sg}) - C_{12}(\phi_h + \phi_g - \beta_h - \beta_g) + C_i(\dot{X}_{sh} + \dot{X}_{sg}) + C_i\omega(Y_{sh} + Y_{sg}) = f_{1h}, \tag{A.1}$$

$$M_2(\ddot{Y}_{2h} + \ddot{Y}_{2g}) + K_s(Y_{sh} + Y_{sg}) - C_{12}(\theta_h + \theta_g - \alpha_h - \alpha_g) + C_i(\dot{Y}_{sh} + \dot{Y}_{sg}) - C_i\omega(X_{sh} + X_{sg}) = f_{2h} - f_{2g}, \tag{A.2}$$

$$(K(X_{JL}))_L(X_{JLh} + X_{JLg}) - K_s(X_{sh} + X_{sg})e_2 - C_i(\dot{X}_{sh} + \dot{X}_{sg})e_2 - C_i\omega(Y_{sh} + Y_{sg})e_2 + C_{22}(\phi_h + \phi_g - \beta_h - \beta_g)/l + C_{12}(\phi_h + \phi_g - \beta_h - \beta_g)e_2 - C_{12}/l(X_{sh} + X_{sg}) = 0, \tag{A.3}$$

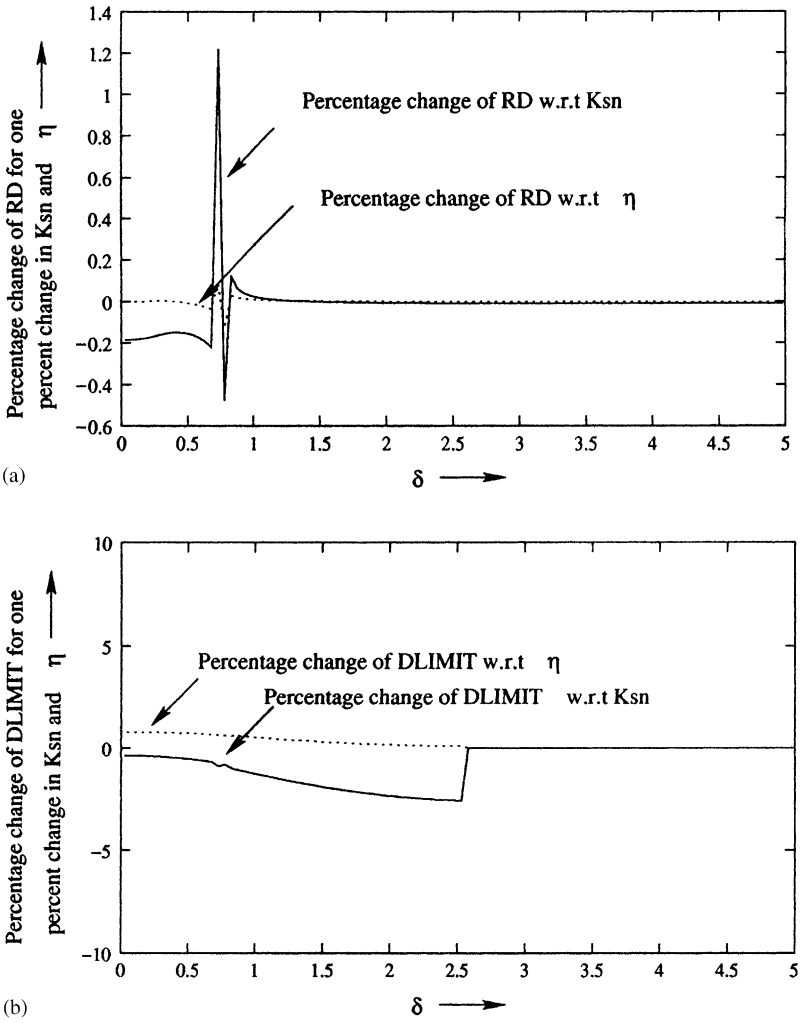

Fig. 7. (a), (b) Sensitivity plots for *RD* minimization and (c), (d) sensitivity plots for (*RD-DLIMIT*) minimization.

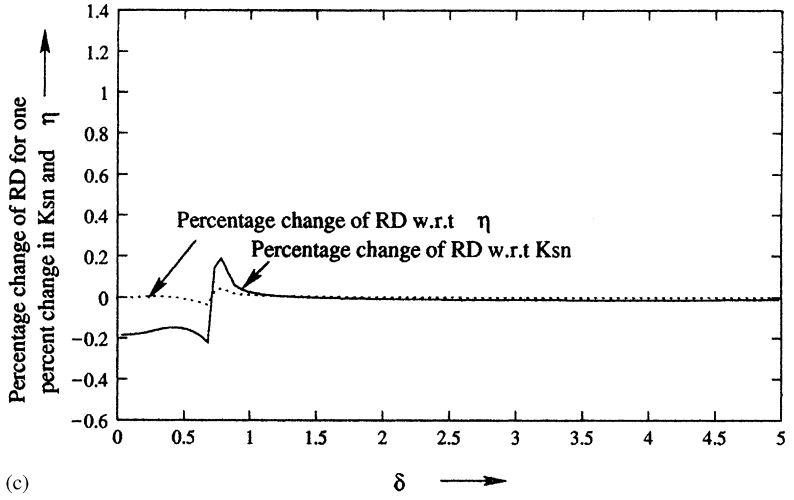

(c)

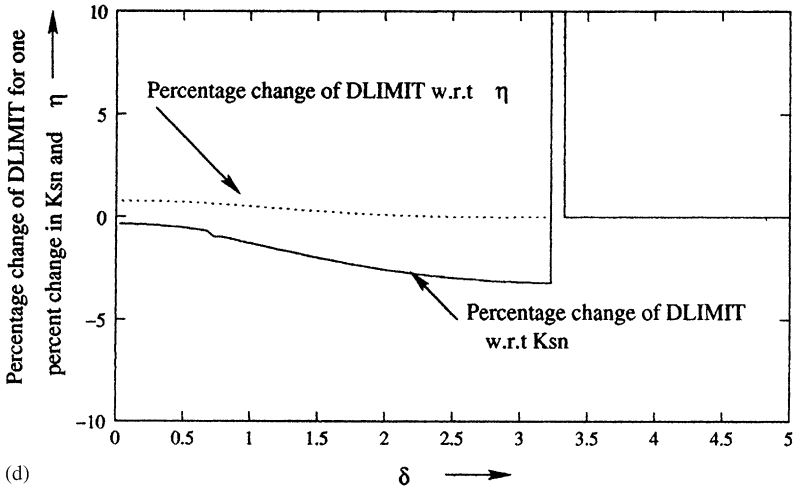

(d)

Fig. 7 (*continued*).

$$(K(Y_{JL}))_L(Y_{JLh} + Y_{JLg}) - K_s(Y_{sh} + Y_{sg})e_2 - C_i(\dot{Y}_{sh} + \dot{Y}_{sg})e_2 - C_i\omega(X_{sh} + X_{sg})e_2 + C_{22}(\theta_h + \theta_g - \alpha_h - \alpha_g)/l + C_{12}(\theta_h + \theta_g - \alpha_h - \alpha_g)e_2 - C_{12}/l(Y_{sh} + Y_{sg}) = 0, \quad \text{(A.4)}$$

$$(K(X_{JR}))_R(X_{JRh} + X_{JRg}) - K_s(X_{sh} + X_{sg})e_1 - C_i(\dot{X}_{sh} + \dot{X}_{sg})e_1 - C_i\omega(Y_{sh} + Y_{sg})e_1 - C_{22}(\phi_h + \phi_g - \beta_h - \beta_g)/l + C_{12}(\phi_h + \phi_g - \beta_h - \beta_g)e_1 + C_{12}/l(X_{sh} + X_{sg}) = 0, \quad \text{(A.5)}$$

$$(K(Y_{JR}))_R(Y_{JRh} + Y_{JRg}) - K_s(Y_{sh} + Y_{sg})e_1 - C_i(\dot{Y}_{sh} + \dot{Y}_{sg})e_1 - C_i\omega(X_{sh} + X_{sg})e_1 - C_{22}(\theta_h + \theta_g - \alpha_h - \alpha_g)/l + C_{12}(\theta_h + \theta_g - \alpha_h - \alpha_g)e_1 + C_{12}/l(Y_{sh} + Y_{sg}) = 0, \quad \text{(A.6)}$$

$$M_1(\ddot{X}_{1Lh}+\ddot{X}_{1Lg})-K_s(X_{sh}+X_{sg})e_2+C_{22}(\phi_h+\phi_g-\beta_h-\beta_g)/l+K_1(X_{1Lh}+X_{1Lg})+C_1(\dot{X}_{1Lh}+\dot{X}_{1Lg})+K_2(X_{1Lh}+X_{1Lg}-X_{3Lh}-X_{3Lg})+C_{12}(\phi_h+\phi_g-\beta_h-\beta_g)e_2-C_{12}/l(X_{sh}+X_{sg})-C_i(\dot{X}_{sh}+\dot{X}_{sg})e_2-C_i\omega Y_s e_2=0, \tag{A.7}$$

$$M_1(\ddot{Y}_{1Lh}+\ddot{Y}_{1Lg})-K_s(Y_{sh}+Y_{sg})e_2+C_{22}(\theta_h+\theta_g-\alpha_h-\alpha_g)/l+K_1(Y_{1Lh}+Y_{1Lg})+C_1(\dot{Y}_{1Lh}+\dot{Y}_{1Lg})+K_2(Y_{1Lh}+Y_{1Lg}-Y_{3Lh}-Y_{3Lg})+C_{12}(\theta_h+\theta_g-\alpha_h-\alpha_g)e_2-C_{12}/l(Y_{sh}+Y_{sg})-C_i(\dot{X}_{sh}+\dot{X}_{sg})e_2+C_i\omega(X_{sh}+X_{sg})e_2=-f_{3g}, \tag{A.8}$$

$$M_1(\ddot{X}_{1Rh}+\ddot{X}_{1Rg})-K_s(X_{sh}+X_{sg})e_1-C_{22}(\phi_h+\phi_g-\beta_h-\beta_g)/l+K_1(X_{1Rh}+X_{1Rg})+C_1(\dot{X}_{1Rh}+\dot{X}_{1Rg})+K_2(X_{1Rh}+X_{1Rg}-X_{3Rh}-X_{3Rg})+C_{12}(\phi_h+\phi_g-\beta_h-\beta_g)e_1+C_{12}/l(X_{sh}+X_{sg})-C_i(\dot{X}_{sh}+\dot{X}_{sg})e_1-C_i\omega(Y_{sh}+Y_{sg})e_1=0, \tag{A.9}$$

$$M_1(\ddot{Y}_{1Rh}+\ddot{Y}_{1Rg})-K_s(Y_{sh}+Y_{sg})e_1-C_{22}(\theta_h+\theta_g-\alpha_h-\alpha_g)/l+K_1(Y_{1Rh}+Y_{1Rg})+C_1(\dot{Y}_{1Rh}+\dot{Y}_{1Rg})+K_2(Y_{1Rh}+Y_{1Rg}-Y_{3Rh}-Y_{3Rg})+C_{12}(\theta_h+\theta_g-\alpha_h-\alpha_g)e_1+C_{12}/l(Y_{sh}+Y_{sg})-C_i(\dot{Y}_{sh}+\dot{Y}_{sg})e_1-C_i\omega(X_{sh}+X_{sg})e_1=-f_{3g}, \tag{A.10}$$

$$M_3(\ddot{X}_{3Lh}+\ddot{X}_{3Lg})+K_2(X_{3Lh}+X_{3Lg}-X_{1Lh}-X_{1Lg})+C_2(\dot{X}_{3Lh}+\dot{X}_{3Lg})=0, \tag{A.11}$$

$$M_3(\ddot{Y}_{3Lh}+\ddot{Y}_{3Lg})+K_2(Y_{3Lh}+Y_{3Lg}-Y_{1Lh}-Y_{1Lg})+C_2(\dot{Y}_{3Lh}+\dot{Y}_{3Lg})=-f_{4g}, \tag{A.12}$$

$$M_3(\ddot{X}_{3Rh}+\ddot{X}_{3Rg})+K_2(X_{3Rh}+X_{3Rg}-X_{1Rh}-X_{1Rg})+C_2(\dot{X}_{3Rh}+\dot{X}_{3Rg})=0, \tag{A.13}$$

$$M_3(\ddot{Y}_{3Rh}+\ddot{Y}_{3Rg})+K_2(Y_{3Rh}+Y_{3Rg}-Y_{1Rh}-Y_{1Rg})+C_2(\dot{Y}_{3Rh}+\dot{Y}_{3Rg})=-f_{4g}, \tag{A.14}$$

$$I_t(\ddot{\phi}_h+\ddot{\phi}_g)+C_{22}(\phi_h+\phi_g-\beta_h-\beta_g)+I_p\omega(\dot{\theta}_h+\dot{\theta}_g)-C_{12}(X_{sh}+X_{sg})=0, \tag{A.15}$$

$$I_t(\ddot{\theta}_h+\ddot{\theta}_g)+C_{22}(\theta_h+\theta_g-\alpha_h-\alpha_g)-I_p\omega(\dot{\phi}_h+\dot{\phi}_g)-C_{12}(Y_{sh}+Y_{sg})=0, \tag{A.16}$$

where $f_{1h}=M_2e_u\omega^2\cos(\omega t)$, $f_{2h}=M_2e_u\omega^2\sin(\omega t)$, $f_{2g}=M_2g$, $f_{3g}=M_1g$, $f_{4g}=M_3g$. All time derivatives of the terms with subscript 'g' are zero, since these terms are constants.

A.2. In non-dimensional form

$$\delta^2(x_{2h}+x_{2g})+A_1(x_{sh}+x_{sg})-A_2(\phi'_h+\phi'_g-x_{ash}-x_{asg})+2\zeta_i\delta(x_{sh}+x_{sg})+2\zeta_i\delta(y_{sh}+y_{sg})=\delta^2, \tag{A.17}$$

$$\delta^2(y_{2h}+y_{2g})+A_1(y_{sh}+y_{sg})-A_2(\theta'_h+\theta'_g-y_{ash}-y_{asg})+2\zeta_i\delta(y_{sh}+y_{sg})-2\zeta_i\delta(x_{sh}+x_{sg})=-\mathrm{i}\delta^2, \tag{A.18}$$

$$(\beta(x_{JL}))_L(x_{JLh}+x_{JLg})-A_1e_2(x_{sh}+x_{sg})-2\zeta_i\delta e_2(x_{sh}+x_{sg})-2\zeta_i\delta e_2(y_{sh}+y_{sg})+A_3(\phi'_h+\phi'_g-x_{ash}-x_{asg})+A_2(\phi'_h+\phi'_g-x_{ash}-x_{asg})e_2-A_2(x_{sh}+x_{sg})=0, \tag{A.19}$$

$$(\beta(y_{JL}))_L(y_{JLh}+y_{JLg})-A_1e_2(y_{sh}+y_{sg})-2\zeta_i\delta e_2(y_{sh}+y_{sg})+2\zeta_i\delta e_2(x_{sh}+x_{sg})+A_3(\theta'_h+\theta'_g-y_{ash}-y_{asg})+A_2(\theta'_h+\theta'_g-y_{ash}-y_{asg})e_2-A_2(y_{sh}+y_{sg})=0, \tag{A.20}$$

$$(\beta(x_{JR}))_R(x_{JRh}+x_{JRg})-A_1e_1(x_{sh}+x_{sg})-2\zeta_i\delta e_1(x_{sh}+x_{sh})-2\zeta_i\delta e_1(y_{sh}+y_{sh})-A_3(\phi'_h+\phi'_g-x_{ash}-x_{asg})+A_2(\phi'_h+\phi'_g-x_{ash}-x_{asg})e_1+A_2(x_{sh}+x_{sg})=0, \tag{A.21}$$

$$(\beta(y_{JR}))_R(y_{JRh}+y_{JRg})-A_1e_1(y_{sh}+y_{sg})-2\zeta_i\delta e_1(y_{sh}+y_{sg})+2\zeta_i\delta e_1(x_{sh}+x_{sg})-A_3(\theta'_h+\theta'_g-y_{ash}-y_{asg})+A_2(\theta'_h+\theta'_g-y_{ash}-y_{asg})e_1+A_2(y_{sh}+y_{sg})=0, \tag{A.22}$$

$$\alpha_1\delta^2(x_{1Lh}+x_{1Lg})-A_1e_2(x_{sh}+x_{sg})+A_3(\phi'_h+\phi'_g-x_{ash}-x_{asg})+\beta_1(x_{1Lh}+x_{1Lg})+\beta_2(x_{1Lh}+x_{1Lg}-x_{3Lh}-x_{3Lg})+2\zeta_1\delta(x_{1Lh}+x_{1Lg})+A_2e_2(\phi'_h+\phi'_g-x_{ash}-x_{asg})-A_2(x_{sh}+x_{sg})-2\zeta_i\delta e_2(x_{sh}+x_{sg})-2\zeta_i\delta e_2(y_{sh}+y_{sg})=0, \tag{A.23}$$

$$\alpha_1\delta^2(y_{1Lh}+y_{1Lg})-A_1e_2(y_{sh}+y_{sg})+A_3(\theta'_h+\theta'_g-y_{ash}-y_{asg})+\beta_1(y_{1Lh}+y_{1Lg})+\beta_2(y_{1Lh}+y_{1Lg}-y_{3Lh}+y_{3Lg})+2\zeta_1\delta(y_{1Lh}+y_{1Lg})+A_2e_2(\theta'_h+\theta'_g-y_{ash}-y_{asg})-A_2(y_{sh}+y_{sg})-2\zeta_i\delta e_2(y_{sh}+y_{sg})+2\zeta_i\delta e_2(x_{sh}+x_{sg})=-\alpha_1\gamma, \tag{A.24}$$

$$\alpha_1\delta^2(x_{1Rh}+x_{1Rg})-A_1e_1(x_{sh}+x_{sg})-A_3(\phi'_h+\phi'_g-x_{ash}-x_{asg})+\beta_1(x_{1Rh}+x_{1Rg})+\beta_2(x_{1Rh}+x_{1Rg}-x_{3Rh}-x_{3Rg})+2\zeta_1\delta(x_{1Rh}+x_{1Rg})-A_2e_1(\phi'_h+\phi'_g-x_{ash}-x_{asg})+A_2(x_{sh}+x_{sg})-2\zeta_i\delta e_1(x_{sh}+x_{sg})-2\zeta_ie_1(y_{sh}+y_{sg})=0, \tag{A.25}$$

$$\alpha_1\delta^2(y_{1Rh}+y_{1Rg})-A_1e_1(y_{sh}+y_{sg})-A_3(\theta'_h+\theta'_g-y_{ash}-y_{asg})+\beta_1(y_{1Rh}+y_{1Rg})+\beta_2(y_{1Rh}+y_{1Rg}-y_{3Rh}-y_{3Rg})+2\zeta_1\delta(y_{1Rh}+y_{1Rg})+A_2e_1(\theta'_h+\theta'_g-y_{ash}-y_{asg})-A_2(y_{sh}+y_{sg})-2\zeta_i\delta e_1(y_{sh}+y_{sg})+2\zeta_i\delta e_1(x_{sh}+x_{sg})=-\alpha_1\gamma, \tag{A.26}$$

$$\alpha_2\delta^2(x_{3Lh}+x_{3Lg})+\beta_2(x_{3Lh}+x_{3Lg}-x_{1Lh}-x_{1Lg})+2\zeta_2\delta(x_{3Lh}+x_{3Lg})=0, \tag{A.27}$$

$$\alpha_2\delta^2(y_{3Lh}+y_{3Lg})+\beta_2(y_{3Lh}+y_{3Lg}-y_{1Lh}-y_{1Lg})+2\zeta_2\delta(y_{3Lh}+y_{3Lg})=-\alpha_2\gamma, \tag{A.28}$$

$$\alpha_2\delta^2(x_{3Rh}+x_{3Rg})+\beta_2(x_{3Rh}+x_{3Rg}-x_{1Rh}-x_{1Rg})+2\zeta_2\delta(x_{3Rh}+x_{3Rg})=0, \tag{A.29}$$

$$\alpha_2\delta^2(y_{3Rh}+y_{3Rg})+\beta_2(y_{3Rh}+y_{3Rg}-y_{1Rh}-y_{1Rg})+2\zeta_2\delta(y_{3Rh}+y_{3Rg})=-\alpha_2\gamma, \tag{A.30}$$

$$A_3\delta^2c^2(\phi'_h+\phi'_g)+A_3(\phi'_h+\phi'_g-x_{ash}-x_{asg})+RA_3\delta^2c^2(\theta'_h+\theta'_g)-A_2(x_{sh}+x_{sg})=0, \tag{A.31}$$

$$A_3\delta^2c^2(\theta'_h+\theta'_g)+A_3(\theta'_h+\theta'_g-y_{ash}-y_{asg})-RA_3\delta^2c^2(\phi'_h+\phi'_g)-A_2(y_{sh}+y_{sg})=0, \tag{A.32}$$

where $x_{as}=(x_{JR}+x_{1R}-x_{JL}-x_{1L})$, $y_{as}=(y_{JR}+y_{1R}-y_{JL}-y_{1L})$, x_{as} and y_{as} with their harmonic and gravitational part can be written as $(x_{ash}+x_{asg})$ and $(y_{ash}+y_{asg})$, respectively. $\phi'=\phi l, \theta'=\theta l, A_1=(e_1^2+e_2^2-e_1e_2)/e_1e_2, A_2=(e_1-e_2)$ and $A_3=e_1e_2$.

Appendix B. Nomenclature

α	angular orientations of rotor axis about x-axis
β	angular orientations of rotor axis about y-axis
C_r	deflection due to preload
C_1 and C_2	primary and secondary support damping of each support
C_i	internal damping coefficient
C_{12}	force/angular deflection or moment/deflection of the shaft at rotor disc location, i.e., $K^*l(e_2-e_1)$
C_{22}	moment/angular deflection or angular stiffness of the shaft at rotor disc location, i.e., $K^*l^2(e_1-e_2)$
$\dot{}$	$= \mathrm{d}/\mathrm{d}t$
D	dissipation function
$\langle e \rangle$	error function
e_u	eccentricity at rotor disc
E	Young's modulus of elasticity for shaft material
F	force matrix
f	amplitude of force
g	acceleration due to gravity
I_p and I_t	polar and transverse moments of inertia of the disc
i	$=\sqrt{-1}$
K_s	Stiffness of the shaft at rotor location in transverse plane
K^*	$= 3EII/(l_1^2 l_2^2)$
K_{support}	$= (K_1K_2 + \mathrm{i}\omega(K_1C_2 + K_2C_1 + K_2C_2) - C_1C_2\omega^2)/(K_2 + \mathrm{i}\omega C_2)$ is the complex support stiffness can also be written as $K_{su}(1 + \mathrm{i}\eta)$ where K_{su} is inphase support stiffness and η is the loss factor
$(K_{b,lin})_L$ and $(K_{b,lin})_R$	linearized stiffness of the rolling element bearings at left and right side
K_1 and K_2	primary and secondary support stiffness of each support
l_1 and l_2	distance of rotor disc from left and right bearing
l	length of the shaft
M_1, M_2 and M_3	support mass, mass of the rotor and mass of the viscoelastic element
t	tune in seconds
T and V	kinetic and potential energy
θ	absolute angular deflections of rotor axis about x-axis
ϕ	absolute angular deflections of rotor axis about y-axis
ω	angular velocity of the rotor
ω_n	fundamental undamped natural frequency of the system $\sqrt{K^*/M_2}$
$\{Q\}$	displacement vector
$\{q\}$	amplitude vector of displacements $\{Q\}$
T_s	time period of the shaft

Non-dimensional terms

α_1	mass ratio (M_1/M_2)
α_2	mass ratio (M_3/M_2)
β_b	non-dimensional bearing stiffness (K_b/K^*)
β_0 and β_{cr}	$= K_b(0)/K^*$ and $K_b(C_r)/K^*$
c_r	$= C_r/e_u$
β_1 and β_2	$= K_1/K^*$ and K_2/K^*
$(\beta_{b,lin})_L$, $(\beta_{b,lin})_R$	$= (K_{b,lin})_L/K^*$, $(K_{b,lin})/K^*$
DLIMIT	non-dimensional stability limit (SLS divided by ω_n)
δ	ω/ω_n, i.e., the non-dimensional speed of rotation of the rotor disc
e_1 and e_2	l_1/l and l_2/l
R	I_p/I_t
RD	non-dimensional response (i.e., $\lvert z_2\rvert$)
K_{sn}	non-dimensional in phase support stiffness (i.e., Real$(K_{support})/K^*$) $(= \beta_1\beta_2^2 + 4\delta\zeta_2^2(\beta_1+\beta_2)/(\beta_2^2 + a\delta^2\zeta_2^2))$
η	loss factor of support and is given as Imag$(K_{support})$/ Real$(K_{support})$ $\left(= \frac{2\delta\beta_2^2(\zeta_1+\zeta_2)+8\zeta_1\zeta_2^2\delta^3}{\beta_1\beta_2^2+4\delta^2\zeta_2^2(\beta_1+\beta_2)}\right)$
γ	$= g/(e_u\omega_n^2)$ non-dimensional gravity
ζ_i.	$= C_i/C_c$
ζ_1 and ζ_2	$= C_1/C_c$ and C_2/C_c

References

[1] K.C. Panda, J.K. Dutt, Design of optimum support parameters for minimum rotor response and maximum stability limit speed, Journal of Sound and Vibration 223 (1) (1999) 1–21.

[2] K.M. Ragulskis, et al., Vibration of Bearings, Mintris Publishers, Vilnyus, 1975.

[3] T.A. Harris, Rolling Bearing Analysis, 3rd Edition, Wiley-Interscience, New York, 1966.

[4] G. Genta, A. Repaci, Circular whirling and unbalance response of non-linear rotors, Proceedings of the American Society of Mechanical Engineers Conference on Mechanical Vibration and Noise, Boston, MA, 1987.

[5] O. Robert, P.E. Parsley, Mechanical Components Hand Book, McGraw-Hill, New York, 1985.

[6] S. Saito, Calculation of nonlinear unbalance response of horizontal Jeffcott rotors supported by ball bearings with radial clearances, Journal of Vibration, Acoustics, Stress and Reliability in Design 107 (1985) 416–420.

[7] G. Geneta, F. De Bona, Unbalance response of rotors: a modal approach with some extensions to damped natural systems, Journal of Sound and Vibration 140 (1) (1990) 129–153.

[8] K. Bhattacharaya, J.K. Dutt, Unbalance response and stability analysis of horizontal rotor system mounted on non-linear rolling element bearings with viscoelastic supports, Journal of Vibration and Acoustics 119 (1997) 539–544.

[9] M. Darlow, E. Zorzi, Mechanical Design Hand Book for Elastomers, NASA, CR 3423, 1981.

[10] J.K. Dutt, B.C. Nakra, Stability of rotor systems with viscoelastic supports, Journal of Sound and Vibration 153 (1) (1992) 89–96.

[11] J.K. Dutt, B.C. Nakra, Vibration response reduction of a rotor shaft system using viscoelastic polymeric supports, Journal of Vibration and Acoustics 116 (1993) 221–223.

[12] Corsaro and Sperling, Sound and Vibration Damping with Polymers, ACS Symposium Series, Vol. 424, American Chemical Society, 1990.

[13] W.H. Press, et al., Numerical Recipes in Fortran, Cambridge University Press, Cambridge, 1992.
[14] B.S. Garbow, et al., Matrix Eigen System Routines—EISPACK Guide Extension, Lecture Notes in Computer Science, Springer, Berlin, 1977.
[15] A.D. Nashif, D.I.G. Jones, J.P. Henderson, Vibration Damping, Wiley-Interscience, New York, 1985.
[16] S.S. Rao, Optimization Theory and Application, Wiley Eastern, New York, 1992.